JOURNAL OF SOLID STATE CHEMISTRY **127,** 211–221 (1996)
ARTICLE NO. 0377

Polymorphism and Superstructure in $BaCoS_{2-\delta}$

M. C. Gelabert,* N. E. Brese,† F. J. DiSalvo,*,[1] S. Jobic,‡ P. Deniard,‡ and R. Brec‡

*Department of Chemistry, Cornell University, Ithaca, New York 14853–1301; †Rohme Haas Co., Corporate Exploratory, 727 Norristown Rd., P.O. Box 904, Spring House, Pennsylvania 19477-0904; and ‡Laboratoire de Chimie des Solides, IMN, 2 rue de la Houssinière, 44072, Nantes Cedex 03, France

Received June 27, 1996; accepted September 3, 1996

$BaCoS_{2-\delta}$ consists of at least three different polymorphs: two that are stoichiometric and one that is potentially sulfur deficient with $0.0 \leq \delta \leq 0.2$. Two of these polymorphs were investigated here: a tetragonal single crystal $P4/nmm$, $a = 4.568(1)$ Å, $c = 8.942(2)$ Å ($\delta \approx 0$), and polycrystalline powder $Cmma$, $a = 6.4390(3)$ Å, $b = 6.4909(3)$ Å, $c = 8.9379(4)$ Å ($\delta \approx 0.2$). Room temperature TEM studies show that several classes of superstructures exist in the stoichiometric single crystals of this phase; on cooling the TEM diffraction patterns change and become more complex. Temperature-dependent lattice constants of polycrystalline $BaCoS_{2-\delta}$ show anomalies near −60°C. $BaCoS_{2-\delta}$ is a metastable compound that is prepared above 850°C and subsequently quenched. Synthetic studies show that (1) at the preparation temperature $BaCoS_2$ is in equilibrium with S vapor at pressures on the order of an atmosphere, producing a nonstoichiometric phase $BaCoS_{2-\delta}$; (2) adding some excess sulfur can reduce δ to zero; and (3) too much excess sulfur results in partial or complete melting of the system (however, stoichiometric $BaCoS_2$ crystals can be obtained from those melts). Magnetic susceptibility measurements verify that the Co moments order antiferromagnetically at 310 K. At higher temperatures a Curie–Weiss fit to the data gives $\mu_{eff} = 2.14(4)$ μ_B/Co and $\theta = 150(20)$ K; these data are consistent with a low spin state for Co^{2+} (d^7).

INTRODUCTION

In the continued search for ternary alkaline earth metal sulfides, particularly of late transition metals, there has surfaced considerable interest in the unusual behavior of $BaCoS_2$ (1, 2). This phase is one of the three ternaries discovered so far in the Ba–Co–S system, the others being Ba_2CoS_3 (3) and $Ba_6Co_{25}S_{27}$ (4). $BaCoS_2$ has special thermal and structural properties that are not well understood. In addition, its structure and exact chemical composition are still uncertain. There are a number of questions regarding this phase that have not yet been answered in the reports to date.

$BaCoS_2$, a metastable phase that forms above 850°C, is a Mott insulator with a second-order phase transition in the magnetic susceptibility around 310 K (1). It has a structure (Fig. 1) that contains Co atoms in square pyramidal environments. These polyhedra are arranged alternately up and down to make a sheet, and the Ba ions sit in between. The structure can also be viewed as CoS puckered square sheets separated by two distorted BaS rock-salt (100) layers. The structure is slightly distorted from tetragonal $BaNiS_2$ (5) such that the unit cell is monoclinic with $\beta = 90.45°$. Snyder *et al.* (1) solved the structure in the orthorhombic space group *Cmma*, whereas Baenziger *et al.* (2) refined it in the metrically equivalent $P2/n$ space group. Both structural models give almost identical atomic positions. The monoclinic symmetry refinement may appear a little better with a lower reliability factor and smaller residues, but there are also a smaller number of data/number of variables ratio (8.1 as opposed to 14.5), and therefore it is difficult from these data to infer the true symmetry of the phase. Also, the planar sulfur atoms (S2, those in the CoS sheets) have a thermal parameter twice that of the apical sulfur (S1), and this difference may signal further small distortions not yet understood. Table 1 lists the previously reported cell parameters of $BaCoS_2$, along with the monoclinic angles.

On using excess sulfur to grow crystals for single-crystal diffraction studies, it was discovered that the X-ray powder patterns of the ground crystals could be indexed with smaller monoclinic angles ranging from $\beta \approx 90.1$ to 90.3. This suggests that β may be sensitive to sulfur stoichiometry. In addition, when pressed powders were heated, there was some mass loss due to a measurable amount of sulfur in the gas phase. The brown S_2 gas was clearly visible in the quartz tubes at reaction temperature.

In view of the difficulties encountered in the understanding of the stoichiometry and structure of $BaCoS_2$, we have examined these features in more detail. We present electron diffraction, scanning electron microscopy (SEM), single-crystal X-ray diffraction, X-ray powder diffraction, density measurements, and thermal studies to better un-

[1] To whom correspondence should be addressed.

0022-4596/96 $18.00

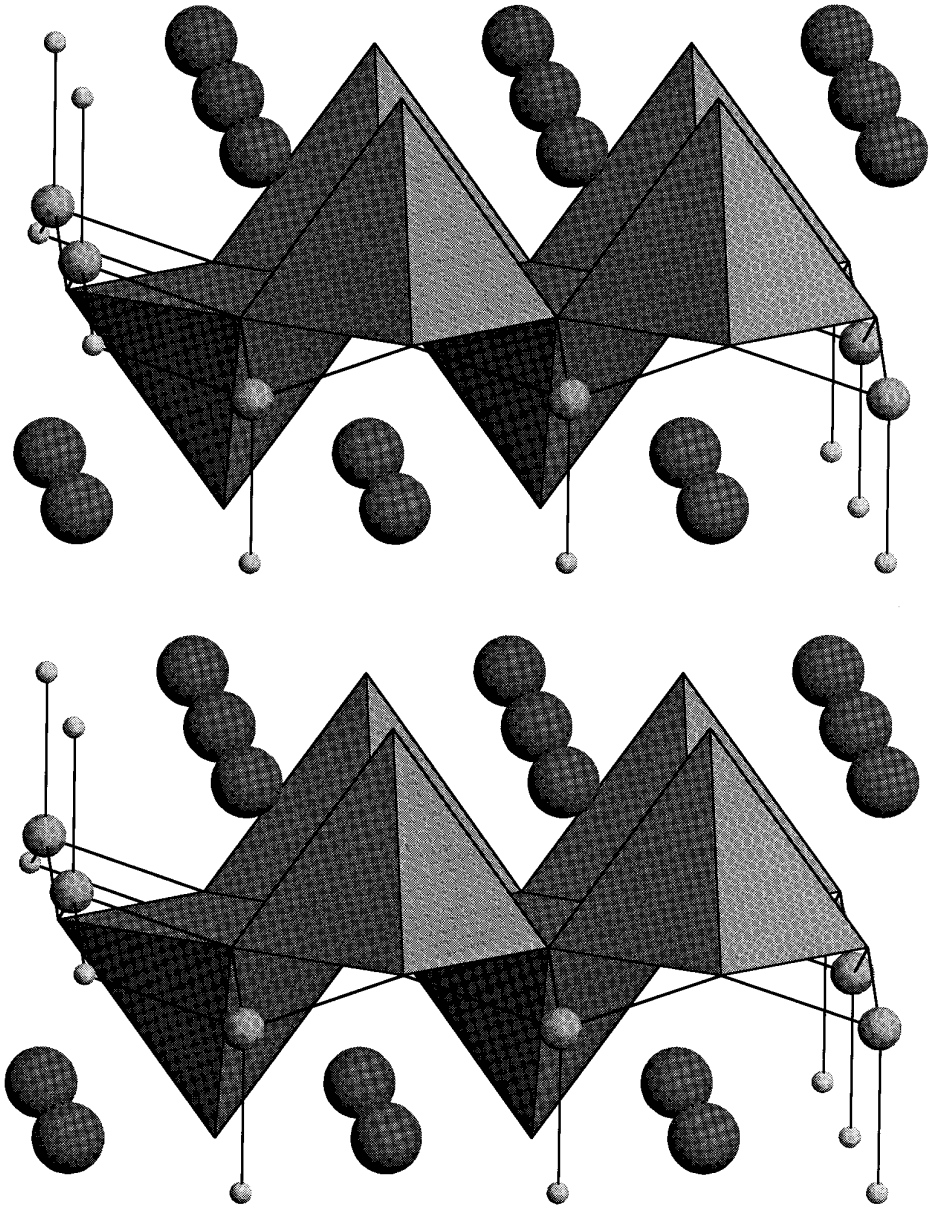

FIG. 1. Approximate structure of $BaCoS_{2-\delta}$. The light small spheres are S, and the dark large spheres are Ba; the rest are Co. The square pyramids represent the coordination of the Co by S.

derstand this very peculiar phase. High-temperature susceptibility measurements have been done to help determine the origin of the magnetic feature at 310 K.

EXPERIMENTAL

Polycrystalline Powder

$BaCoS_{2+x}$ was synthesized by mixing the appropriate molar quantities of the binary sulfides and elemental sulfur (5N). BaS was synthesized from $BaCO_3$ (Johnson Mathey 3N metals basis) following a modified literature procedure (6), and CoS was made from the reaction of Co (Alfa Aesar 4N6) and S (Metalspecialties, 5N5) in an evacuated, sealed quartz tube. A powder mixture of about 0.4 g was ground, pressed into a pellet, and placed into a graphite crucible, which was then sealed in a quartz tube under about 1 Torr of purified argon. The small amount of argon was added to improve thermal contact between the sample and the tube wall, thereby improving the quality of the

TABLE 1
Previously Reported Lattice Constants for $BaCoS_{2-\delta}$

Setting	Snyder *et al.* (1)	Baenziger *et al.* (2)
Orthorhombic		
a_0(Å)	6.4413(3)	—
b_0(Å)	6.4926(3)	—
c_0(Å)	8.9406(4)	—
Monoclinic		
a_m(Å)	4.5729(3)[a]	4.573(3)
b_m(Å)	8.9406(4)	8.937(2)
c_m(Å)	4.5729(3)	4.570(2)
β	90.455(6)	90.43(4)

Note. The orthorhombic cell of Snyder *et al.* has been converted to monoclinic for comparison.

[a] The matrix used to convert the orthorhombic cell of Snyder *et al.* to a monoclinic cell is

$$\begin{pmatrix} a_m \\ b_m \\ c_m \end{pmatrix} = \begin{pmatrix} \frac{1}{2} & \frac{1}{2} & 0 \\ 0 & 0 & -1 \\ -\frac{1}{2} & \frac{1}{2} & 0 \end{pmatrix} \begin{pmatrix} a_0 \\ b_0 \\ c_0 \end{pmatrix}.$$

quench. All the quartz tubes were sealed 6 in. from the bottom of the tube to ensure that the tube volumes are approximately equal. The reaction mixtures were heated to 850–900°C over 12 h in a vertical furnace, held at that temperature for 3–4 days, and finally quenched by dropping the quartz tubes directly out of the bottom of the furnace into an ice water bath.

Room-temperature powder X-ray diffraction for the phase diagram study was done with a Scintag 2000 diffractometer using Cu$K\alpha$ radiation. $K\alpha_2$ stripping and Fourier filtering were used as given in the XDS software, as were peakfinder and deconvolution routines. Lattice constants were calculated using a locally written least-squares program.

Variable-temperature powder X-ray diffraction for Rietveld studies was performed on a Siemens 5000 diffractometer with Cu$K\alpha$ radiation in a Bragg–Brentano geometry. The powder was sifted through several grids to obtain a final particle size of 20 μm. The material was deposited into a cavity at the surface of a flat plate and gently leveled using a frosted glass plate to avoid preferred orientation. The data were collected in steps of 0.02° (2θ) with 50-s counting periods over the range 18–100° 2θ. The powder patterns were processed with the Prolix program (7) including several options such as background stripping, peak search, and profile fitting. Rietveld calculations were carried out on 21 variables and 5379 observations, using the program FULLPROF (8). Recordings of the diffraction diagrams were made from −100 to 200°C in 20° increments. The variable temperature cell constants were refined using the FullPattern matching technique.

Magnetic susceptibility was measured from 4.2 to 773 K in a previously calibrated Faraday microbalance (9). About 60 mg of polycrystalline powder was used for both the low-temperature and high-temperature measurements. X-ray diffraction patterns taken before and after the high-temperature measurement showed ≈1% thermal decomposition into Ba_2CoS_3 and CoS.

Elemental analysis on $BaCoS_2$ was performed by X-ray fluorescence at the Analytical Center of Rhône–Poulenc in Lyon, France. Density measurements were measured with an Accupye 1330 pycnometer in a helium gas environment. Scanning electron microscopy was done with a JEOL 733 microscope with energy-dispersive X-ray spectroscopy for semiquantitative analysis.

Single Crystals

Single crystals of $BaCoS_2$ were grown by heating a sample of nominal composition $BaCoS_{2.3}$ to 950°C for 3 days and quenching.

A black square platelet of dimensions 0.22 × 0.35 × 0.04 mm^3 was chosen for X-ray diffraction and mounted on a glass fiber with 5-min epoxy. Single-crystal X-ray diffraction studies were performed on a Siemens P4 four-circle diffractometer, using Mo$K\alpha$ radiation. The structure determination and refinement were performed with SHELXTL software (10). Absorption was corrected analytically by indexing the faces of the crystal.

The diffraction microscopy study was performed using a Philips CM30 instrument operating at 300 kV. For the sample preparation the crystallites were fragmented and dispersed in ethanol, then set on a carbon grid.

RESULTS

$BaCoS_2$–S Phase Diagram

To study the relationship between sulfur content and structure, an intensive synthetic study of samples with nominal composition $BaCoS_{2+x}$ ($0 \leq x \leq 1$) was performed. Three subjects were the main focus: mass loss, monoclinic angle, and identification of the products. Powder diffraction on such samples (Fig. 2) revealed smaller monoclinic angles than for those with beginning composition $BaCoS_{2.0}$. The mass loss tended to increase with nominal sulfur content. Excess sulfur may be present in the vapor phase or in the sample. No free liquid sulfur can be obtained at this temperature, since its equilibrium vapor pressure is in excess of 100 atm and would cause the quartz container to explode. Table 2 shows the nominal $(2 + x)$ and final $(2 - \delta)$ sulfur content, mass loss, and products obtained for all the reactions, as well as measured β values.

As the sulfur content is increased, some liquid formation is observed at the reaction temperatures; at larger x the formation of liquid occurs at lower temperatures. The mo-

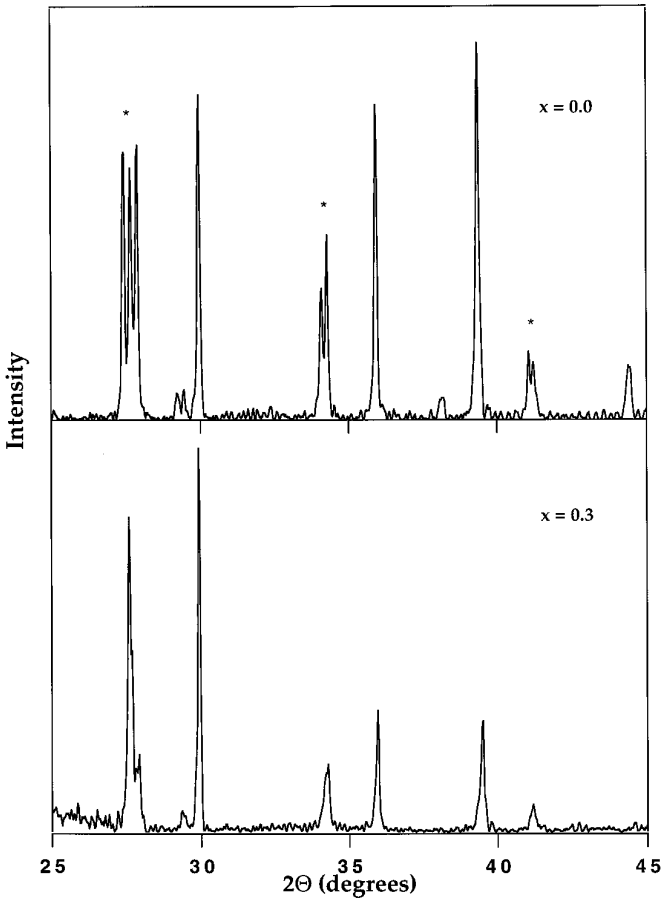

FIG. 2. Partial powder diffraction patterns for $BaCoS_{2+x}$ for $x = 0$ (top) and $x = 0.3$ (bottom). Note the decreased splitting between the starred peaks near 27°, 34°, and 41° 2θ. This visual difference corresponds roughly to a shift in β from 90.5° to 90.1°.

noclinic angle β of the $BaCoS_{2-\delta}$ product also decreases with increasing x; however, larger amounts of sulfur ($x \geq 0.6$) result in the formation of some liquid phase even at the lowest preparation temperatures (850°C) and of multiphase products always including Ba_2CoS_3, BaS, CoS, and $BaCoS_2$. A partial product diagram (Fig. 3) consists then of a $BaCoS_{2-\delta}$–S region at low x and a decomposition region at higher x. The peritectoid line, where $BaCoS_2$ decomposes thermally into Ba_2CoS_3 and CoS on cooling, shifts upward as x increases, crosses the solidus line at about $x = 0.4$, and meets the liquidus at $x \approx 0.6$. The region defined by the liquidus and peritectoid decomposition line is where single-phase $BaCoS_{2-\delta}$ can be obtained. This single-phase region contains both polycrystalline and single-crystalline $BaCoS_2$, with the ratio of the two increasing with x. Past this region, considerable melting occurs and a sharp drop in sulfur vapor pressure and a corresponding increase in average sulfur content of the products are observed. The products contain binary phases and Ba_2CoS_3 as well as single crystals of $BaCoS_2$. These products presumably precipitate from the melt during the quench. These $BaCoS_2$ crystals grow in a very interesting way: the resulting polycrystalline regions, green in color, are sandwiched between plates of black single-crystalline regions. A SEM image of such a product is shown in Fig. 4. One of these samples ($x = 0.7$ heated at 950°C) was separated into black crystals and polycrystalline pieces, and both were ground into powders. X-ray powder diffraction verified that the polycrystalline part is a mixture of Ba_2CoS_3, BaS, and CoS, and that the black single crystals are $BaCoS_{2-\delta}$ with the same β (90.1) as the bulk powder with $\delta = 0.01$.

Single-Crystal X-Ray Diffraction

Single-crystal data were collected on a crystal from a $BaCoS_{2.3}$ batch after determining the unit cell of dimensions $a = 4.562(1)$, $b = 4.567(2)$, $c = 8.946(3)$, $\alpha = 89.97(2)$, $\beta = 89.97(2)$, $\gamma = 89.90(2)$ from rotation photograph reflections. The possible Laue symmetry as determined from the diffractometer software was $4/mmm$ or mmm. The values of the internal R factors were about the same for the averaging of the equivalent symmetry in both classes. Data were collected over slightly more than a quarter of the Ewald sphere, $-1 < h < 6$, $-1 < k < 6$, and $-12 < l < 12$.

TABLE 2
Synthesis Results for $BaCoS_{2+x}$

Temperature (°C)	$S_{initial}$ $(2 + x)$	Mass loss (mg)	S_{final} $(2 - \delta)$	β	Product
850	2.20(2)	6.2(5)	2.06(3)	—	Ba_2CoS_3 + CoS
	2.40	11.8	2.15	—	Ba_2CoS_3 + CoS
	3.00	40.7	2.23	—	dec[a]
900	2.08	8.1	1.91	90.5(1)	112[b]
	2.10	5.9	1.97	90.3	112
	2.20	8.2	2.03	90.3	112
	2.30	18.7	1.95	90.1	112
	2.40	14.3	2.10	—	dec
	2.60	17.4	2.24	—	dec
	2.80	17.8	2.43	90.1	112 + dec
950	2.00	2.0	1.95	90.5	112
	2.20	10.0	2.03	90.2	112
	2.60	49.0	1.98	90.2	112
	2.70	65.0	1.99	90.1	112 + dec
	2.80	16.8	2.44	—	112 + dec
	2.90	20.2	2.48	—	112 + dec

Note. $S_{initial}$ and S_{final} correspond to the sulfur content before and after reacting, respectively, based on mass loss. Lattice constants and product were determined from X-ray powder diffraction.

[a] dec = Ba_2CoS_3 + CoS + BaS.

[b] 112 = $BaCoS_2$.

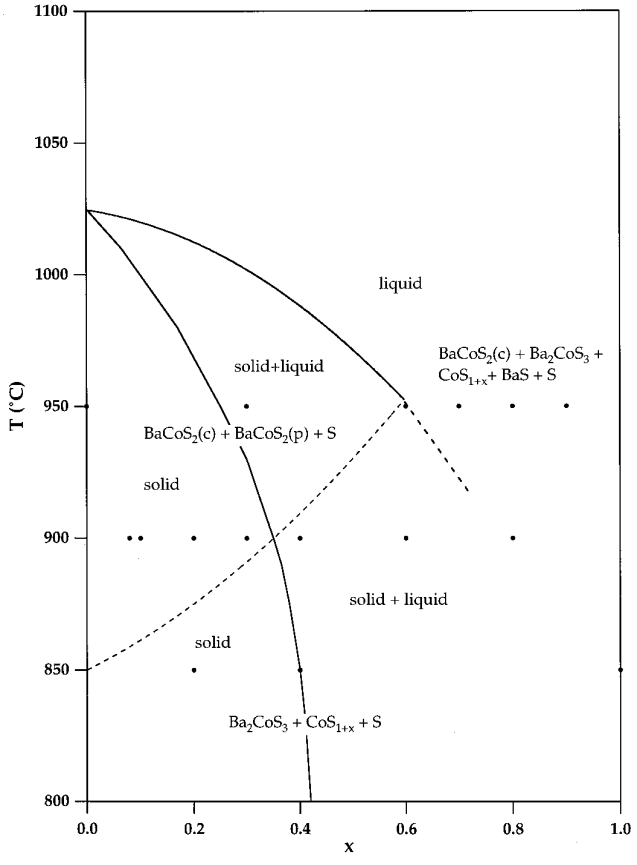

FIG. 3. $BaCoS_{2+x}$ product diagram. The filled circles indicate initial compositions of reactants. For products, c = single crystals and p = polycrystalline powder.

The structure was refined in the space groups *P*4/*nmm* and *Cmma.* Table 3 lists the parameters of the data collection and of the refinements, and Table 4 atomic positions and U_{eq} for *P*4/*nmm*. The atomic coordinates and thermal parameters obtained for both space groups are within experimental error.

The refinements for both space groups *P*4/*nmm* and *Cmma* are quite similar. The S2 atom continues to have a larger thermal parameter, in agreement with what has been reported previously (1, 2). Freeing of the occupancy ratio of all atoms did not result in any significant change [the occupancy factor $\tau = 1.0(1)$ for all atoms]. Since S2 has strong U_{11} and U_{22} values, the structure was refined using eightfold positions for this atom, with an occupancy ratio of 0.5. This did not improve the refinement. It seems that the high S2 thermal parameter is intrinsic to the phase, and there is no single explanation for it using the diffraction data alone. It is useful to note, however, that both sulfur atoms in $BaNiS_2$ also show some differences in the thermal parameters ($B_{eq} = 0.97$ for S1 and 0.57 for S2) (5), in the opposite sense to that which we have observed in $BaCoS_2$.

The crystal data indicate stoichiometric $BaCoS_2$ with either an orthorhombic or tetragonal symmetry.

Powder X-Ray Diffraction

The structure of $BaCoS_{2-\delta}$ ($x = 0$, $\delta \approx 0.04$ determined from mass loss) was refined from powder diffraction data. The powder patterns always show splittings of the (11*l*) tetragonal reflections, clearly indicating the broken tetragonal symmetry. The Bravais lattice in this case is centered orthorhombic, which is metrically equivalent to a monoclinic primitive cell. In the orthorhombic symmetry the lattice parameters were found to be $a = 6.4390(3)$ Å, $b = 6.4909(3)$ Å, and $c = 8.9379(4)$ Å. The fact that this powder and the above crystal are different materials is obvious because of this splitting and because the reflection lines cannot be accounted for using previously measured single-crystal lattice constants. The structure was refined using Rietveld methods in the *Cmma* space group.

The atomic structure refinement (Table 5) was performed by fixing the B_{eq} of both S1 and S2 to 1.0 Å^2, approximately the same value as that determined in the

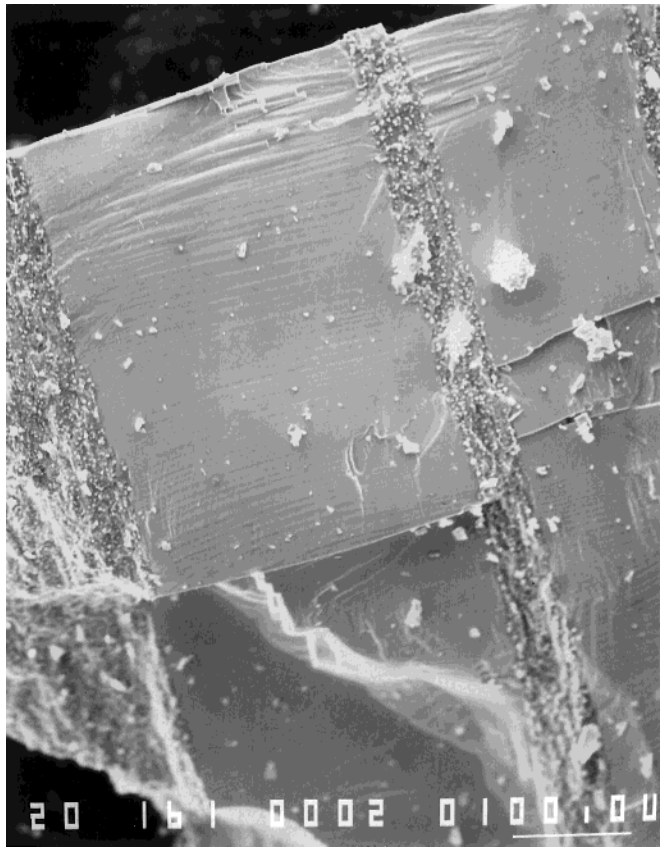

FIG. 4. SEM photograph of a sample with $x = 0.7$ and $\delta \approx 0.01$. The smooth regions are black, single crystalline $BaCoS_2$; the rough regions are green and polycrystalline (CoS + BaS + Ba_2CoS_3).

TABLE 3
Single-Crystal Data Parameters and Refinement for $BaCoS_2$

Empirical formula	$BaCoS_2$	
Formula weight	260.39	
Temperature	293(2) K	
Wavelength	0.71073 Å	
Crystal size	$0.35 \times 0.22 \times 0.04$ mm^3	
Crystal indices	{110}, {−110}, {001}, {−100}	
Cell for data collection	$a = 4.562(1)$, $\alpha = 89.97(2)$	
	$b = 4.567(1)$, $\beta = 89.97(2)$	
	$c = 8.946(3)$, $\gamma = 89.90(2)$	
θ range for data collection	2.28°–29.98°	
Limiting indices	$-1 \le h \le 6$, $-1 \le k \le 6$, $-12 \le l \le 12$	
Reflections collected	798	
Absorption correction	Integration	
Maximum and minimum transmission	0.4435 and 0.1044	
Refinement method	Full-matrix least-squares on F^2	
Crystal system	Tetragonal	Orthorhombic
Space group	*P*4/*nmm*	*Cmma*
Unit cell dimensions	$a = 4.568(1)$ Å	$a = 6.450(1)$ Å
		$b = 6.461(1)$ Å
	$c = 8.942(2)$ Å	$c = 8.946(2)$ Å
Volume, Z	186.59(5) Å^3, 2	372.8(1) A^3, 4
Calculated density	4.635 g/cm^3	4.640 g/cm^3
Absorption coefficient	15.782 mm^{-1}	15.800 mm^{-1}
$F(000)$	230	460
Independent reflections	194 ($R_{int} = 0.0469$)	249 ($R_{int} = 0.0440$)
Data/restraints/parameters	194/0/13	249/0/17
Goodness-of-fit on F^2	1.034	1.241
Final R indices [$I > 2\sigma(I)$]	$R_1 = 0.0250$, $wR_2 = 0.1117$	$R_1 = 0.0223$, $wR_2 = 0.0578$
R indices (all data)	$R_1 = 0.0256$, $wR_2 = 0.1126$	$R_1 = 0.0238$, $wR_2 = 0.0583$
Extinction coefficient	0.06(2)	0.015(2)
Largest diffraction peak and hole	1.651, −1.102 e/Å^3	1.038, −0.859 e/Å^3

single-crystal study for the apical S1. They were kept fixed during the refinement, the assumption made that S2 was behaving in a normal way. The B_{eq} for Co and Ba were also fixed to single-crystal values because they proved difficult to stabilize in the powder refinement. The occupancy ratio of S2 was set free (the B_{eq} and τ variables are too correlated in Rietveld refinements to be varied simultaneously). Attempts to refine B_{eq} with a completely filled S2 site resulted in negative thermal parameters ($B_{eq} \approx -1.5$ Å^2).

TABLE 4
Atomic Coordinates and Thermal Parameters from the Single-Crystal Data Refinement in Space *P*4/*nmm*

Atom	x	y	z	U_{eq} ($\times 10^3$ Å^2)
Ba	$\frac{1}{4}$	$\frac{1}{4}$	0.6975(5)	14(1)
Co	$\frac{1}{4}$	$\frac{1}{4}$	0.0933(2)	17(1)
S1	$\frac{1}{4}$	$\frac{1}{4}$	0.3488(3)	11(1)
S2	$\frac{3}{4}$	$\frac{1}{4}$	0	32(1)

Clearly, some meaningful nonstoichiometry is evidenced with this material and with the type of calculation chosen here. A Rietveld refinement was done assuming the presence of both the orthorhombic and tetragonal phases; the results indicated at most a 2% fraction of tetragonal $BaCoS_2$. The powder, at least in its majority, is orthorhombic and could be nonstoichiometric. According to the Rietveld analysis, the stoichiometry of the powder compound is $BaCoS_{1.84(1)}$.

Low-Temperature X-Ray Diffraction

The cell parameters versus temperature for $BaCoS_{2-\delta}$ are shown in Fig. 5. All the diagrams are that of the orthorhombic cell, hence the structure type of the compound does not change at all in the temperature range considered. Rietveld analysis did not reveal any meaningful difference between the 25 and −100°C structures; however, a transition does occur at around −60°C, with a clear break in the slope. It may very well be explained by the occurrence of a weak superstructure in the compound, as will be discussed. Interestingly enough, this corresponds to the previously

TABLE 5
Structural Solution from X-ray Powder Diffraction Data Taken at Room Temperature

Molecular formula	$BaCoS_2$
Temperature	293(5) K
Wavelength	1.5406 Å
2θ range for data collection	18°–100°
Step size, time/step	0.02°, 50 s
Observations, variables	5379, 21
Space group	*Cmma*
Cell parameters	a = 6.4390(3) Å
	b = 6.4909(3) Å
	c = 8.9379(4) Å
Profile function	Pseudo-Voigt
χ^2	1.75
R_{wp}	0.0381

Atom	x	y	z	B_{eq} (Å^2)	τ
Ba	0	$\frac{1}{4}$	0.1973(3)	0.99	1
Co	0	$\frac{1}{4}$	0.5895(6)	1.2	1
S1	0	$\frac{1}{4}$	0.8433(9)	1.0	1
S2	$\frac{1}{4}$	$\frac{1}{2}$	$\frac{1}{2}$	1.0	0.84(1)

Note. All the thermal parameters and occupancies (except that of S2) were kept fixed during the S2 occupancy refinement. Note that $B_{eq} = 8\pi^2 U_{eq}$.

recorded phase transition temperature in $BaCo_{0.9}Ni_{0.1}S_{2-y}$. This series of sulfur-deficient phases (not structurally documented) show first-order phase transitions for $0.05 < y < 0.20$, with a maximum change in resistivity at the transition occurring around $y = 0.20$, a sulfur stoichiometry very close to that observed for the $BaCoS_{2-\delta}$ phase studied here (11). The transition for the $BaCo_{0.9}Ni_{0.1}S_{1.80}$ composition is found at around −60°C on cooling (at −40°C on heating due to hysteresis). $BaCoS_{2-\delta}$ shows no such phase transition in the resistivity data (1).

Electron Diffraction Study

The $BaCoS_2$ crystals were laid out flat so that most of the observations could be done of the (110) plane, that which is most likely to be relevant to distinguish the various phases present in the samples. Room and low temperature (−100°C) studies were performed. The room temperature (110) planes showed the occurrence of three different classes. Class I (Fig. 6a) was found to correspond to a 4.5 × 4.5-Å primitive network (6.4 × 6.4 Å in the centered setting). This cell matches either of the symmetries chosen in the previous and above studies. Class II (Fig. 6b) corresponds to a doubling of one of the parameters, say a, with the occurrence of medium-intensity superstructure spots (9.0 × 4.5-Å cell). Class III shows weak superstructure spots (Fig. 6c) doubling both the a and b parameters (9.0 × 9.0-Å cell). On cooling, class I samples led to class II as did class III, which even led to a class II′, that is, a class II diagram with superstructure spot intensities as strong as those of the substructure (Fig. 6d). Note that one crystal could show several classes at a given temperature, since the domains span a few dozens of nanometers.

Elemental Analysis and Density Measurements

Elemental analysis was done on polycrystalline $BaCoS_{2-\delta}$ ($x = 0$, $\delta \approx 0.04$ by mass loss). The average

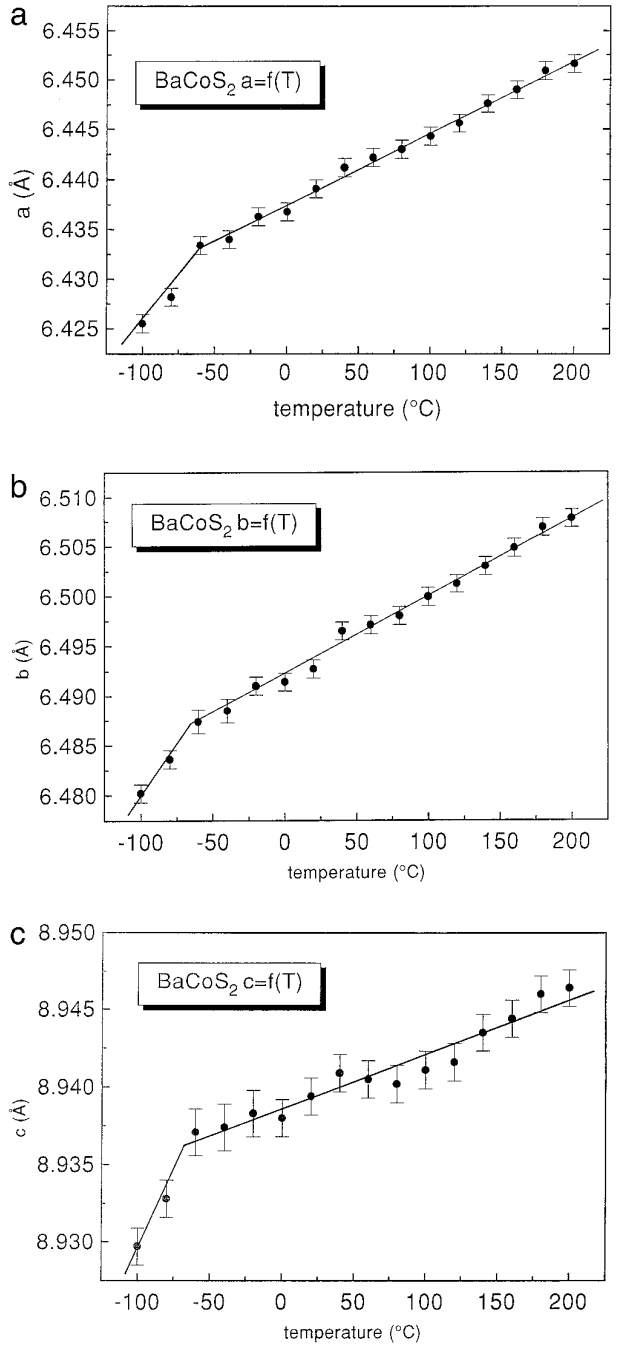

FIG. 5. Orthorhombic lattice parameters a (a), b (b), and c (c) versus temperature for $BaCoS_{2-\delta}$.

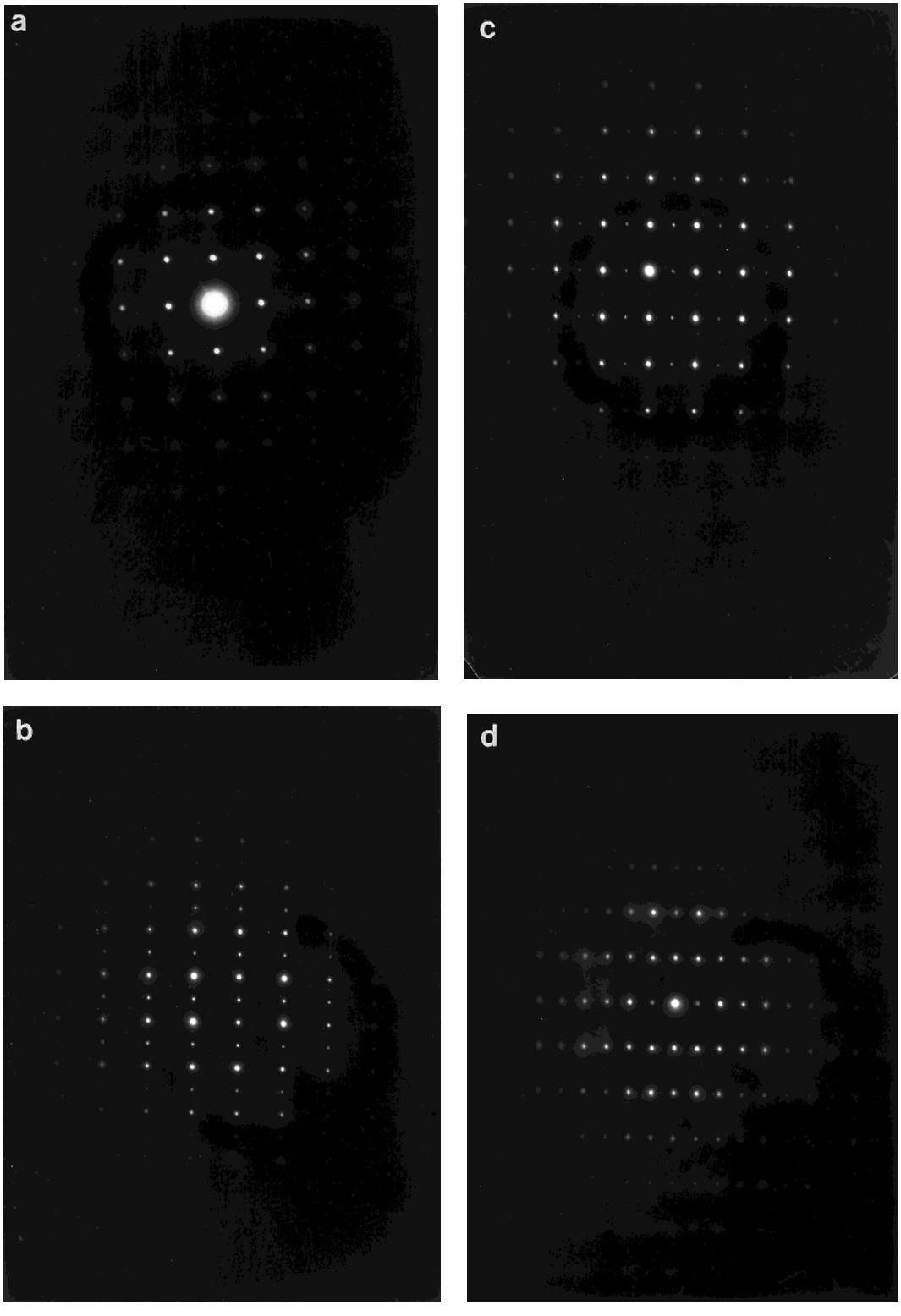

FIG. 6. Electron diffraction photos of a $BaCoS_2$ single crystal. The {001} family of planes are parallel to the page. Classes I, II, and III are all present at room temperature. (a) Class I corresponding to the primitive $a \times a$ lattice. (b) Class II corresponding to a doubling of one of the parameters. (c) Class III corresponding to doubling of both parameters. (d) Class II′ is analogous to class II, except that the intensity of the superstructure spots is enhanced.

percentage compositions obtained were Ba, 52.37; Co, 22.67; S, 23.10. Taking Co as a reference, the calculations yield the formula $Ba_{0.991(6)}Co_{1.00(1)}S_{1.873(5)}$. This result agrees well with the powder refinement on the same sample. To further check this, the density was measured using a very sensitive Accupye 1330 V1.03 helium gas pycnometer. A density of 4.50(3) g/cm^3 was obtained, compared with the theoretical density of 4.63 for an orthorhombic cell containing no atomic defects. This result indicates that there are some vacancies (cation or anion) in the structure. Assuming only sulfur vacancies, the calculated stoichiometry is $BaCoS_{1.78(2)}$, again suggesting a significant sulfur vacancy concentration.

Additional density measurements were done on polycrystalline, single-phase samples of nominal composition $BaCoS_{2.1}$, $BaCoS_{2.2}$, and $BaCoS_{2.3}$. These measured densities [4.57(1), 4.58(1), 4.60(1)] were somewhat higher than that of the $x = 0$ sample. Based on a simple sulfur vacancy model, the calculated δ values are 0.14, 0.13, and 0.09 for $x = 0.1, 0.2$, and 0.3, respectively. These results suggest then that adding excess sulfur shifts the sulfur stoichiometry of the product toward the ideal value of 2.0.

Magnetic Susceptibility

Figure 7 presents magnetic susceptibility data for samples of nominal composition $BaCoS_{2+x}$ ($x = 0$ and $x = 0.1$, both δ values ≈ 0.03 by mass loss). The feature around 310 K is prominent; below this temperature, there is a dropoff in susceptibility with a small tail at 4 K most likely due to a small paramagnetic impurity. Above the transition, the susceptibility drops in a Curie–Weiss fashion. A fit to the Curie–Weiss law, $\chi = \chi_0 + C/(T + \theta)$, over 350–800 K yields $C = 2.2(1) \times 10^{-3}$ emu-K/g, $\mu_{\text{eff}}/\text{Co} = 2.14(4)\ \mu_B$, $\chi_0 = 4.8(1) \times 10^{-6}$ emu/g, and $\theta = 150(20)$ K. From this Curie constant, if a spin of $\frac{1}{2}$ per Co ion is assumed, the Landé g factor is 2.47. On the other hand, if $g = 2$, the calculated spin on the Co is 0.68(2); however, a sulfur deficiency of 10% (composition $BaCoS_{1.8}$) produces a mixture of Co^+/Co^{2+} with composition $BaCo^{2+}_{0.6}Co^{+}_{0.4}S_{1.8}$. If these ions are spin 1 and spin $\frac{1}{2}$, respectively, with $g = 2$ the calculated Co^+ concentration is 0.32, in reasonable agreement with what is expected from the stoichiometry.

To investigate how sulfur content affects the susceptibility, high-temperature magnetic susceptibility from 300 to 800 K was measured for a sample of nominal composition $BaCoS_{2.1}$. The high-temperature behavior was similar to that of the previous sample; fits to the Curie–Weiss law from 350 to 800 K yield $C = 1.6(1) \times 10^{-3}$ emu-K/g, $\mu_{\text{eff}}/\text{Co} = 1.83(4)\ \mu_B$, $\chi_0 = 5.3(1) \times 10^{-6}$ emu/g, and $\theta = 80(20)$. If spin $\frac{1}{2}$ and all Co^{2+} is assumed, then the calculated g is 2.11.

DISCUSSION

The single crystals examined here were separated from a sample prepared at $x = 0.3$ and 950°C. This sample also contained polycrystalline $BaCoS_{2-\delta}$ which had different lattice parameters than the crystal. Obviously then, under these preparation conditions, the product consists of at least two phases. Also, the single-crystal stoichiometry is close to $BaCoS_2$, whereas the powder is sulfur-deficient, with approximate stoichiometry $BaCoS_{1.82}$.

Clearly, the powder diffraction patterns show well-defined, split peaks corresponding to the broken symmetry, so a large majority of monoclinic powder is expected. An electron microscopy study of this powder showed a majority phase and a minority one which could be attributed to $BaCoS_{1.82}$ and $BaCoS_2$, respectively. Also, the various crystals we have studied seemed to belong to the stoichiometric species. This could mean that in the samples, the minority phase is much better crystallized than the majority one: when crystals are sorted out, it is more likely that the stoichiometric ones are selected. From the $BaCo_{1-x}Ni_xS_{2-y}$ series (11) it appears possible to obtain a maximum sulfur deficiency phase at $BaCo_{0.9}Ni_{0.1}S_{1.80}$. This sulfur composition is very close to the nonstoichiometric phase $BaCoS_{1.82}$ that was found in the bulk of the $x = 0$ powder.

We have therefore shown that there are at least two different compositions with slightly differing lattice parameters and symmetry: stoichiometric $BaCoS_2$ and sulfur-deficient phases $BaCoS_{2-\delta}$ with $\delta(\text{max}) \approx 0.2$. With different reaction conditions mass losses suggest that the range of possible sulfur deficiency is $0 < \delta < 0.2$. The primitive cell volumes of all the reported cells are identical within standard deviation. It is of interest to note that Martinson *et al.* have observed the same phenomena within the nonstoichiometric $BaCo_{1-x}Ni_xS_{2-y}$ series (11). They pointed out that there is no evidence of lattice constant changes with y, but the electrical and magnetic properties do show a systematic variation with sulfur vacancies. The substitution of Ni for Co, however, decreases the cell parameter parallel to the a–b plane, whereas the c parameter remains unchanged. In the general case of nonmetallic phases, the parameters may not show the expected lattice expansion on substitution due to lack of long range order. For instance, the cell parameters of $Li_xZrSe_{1.95}$ remain constant up to $x = 0.4$, at which point the phase becomes metallic and the c parameter (the stacking direction) begins to show the expected expansion, the so-called mattress effect (12).

The presence of a superstructure in this material probably accounts for most of the difficulties encountered in the single-crystal X-ray diffraction refinements, perhaps including the inhomogeneity in the S1 and S2 thermal parameters. The appearance of more complex superstructures on cooling could result in a primitive lattice parame-

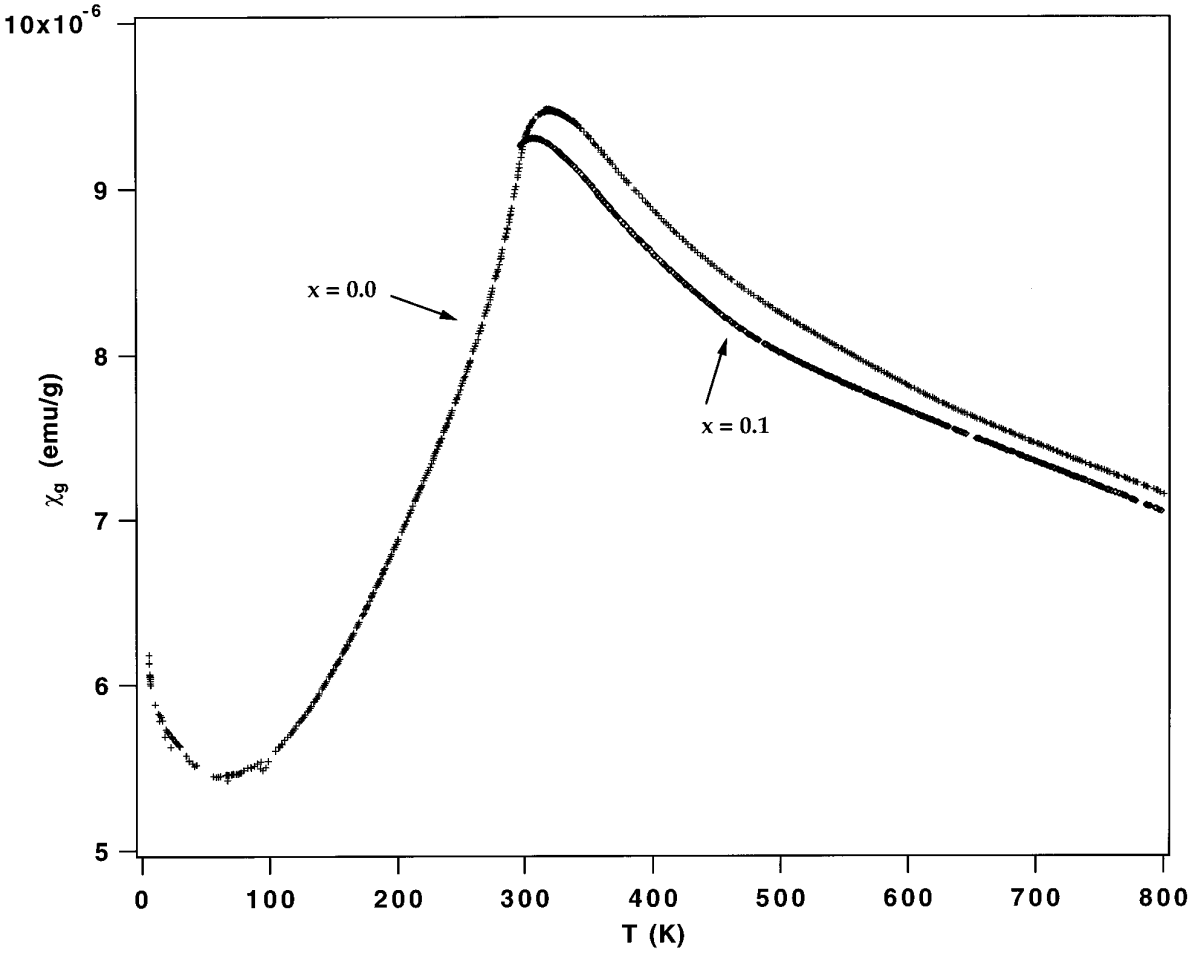

FIG. 7. Magnetic susceptibility of two $BaCoS_{2-\delta}$ polycrystalline powder samples, measured on a Faraday microbalance. Data were obtained for the $x = 0.0$ sample from 4.2 to 800 K; for the $x = 0.1$ sample, 300 to 800 K.

ter shift, and this is what is seen in the low-temperature X-ray powder diffraction patterns.

On synthesis of $BaCoS_{2+x}$ three different processes could take place. First, thermal decomposition occurs below about 850°C at $x = 0$ into Ba_2CoS_3 and CoS; this happens if the material is not taken to the correct temperature or is not properly quenched. Second, single-crystal growth can take place on addition of sulfur, obtaining also polycrystalline $BaCoS_{2-\delta}$ and gaseous sulfur. Finally, at very high x, the product is at least partly molten at the synthesis temperature and a multiphase product is obtained: Ba_2CoS_3, binary phases, and S in addition to single crystals of $BaCoS_2$. In rapidly quenching the sample, more than three phases can be obtained in this three-component system, since the fast quench prevents equilibrium from being achieved due to the slow kinetics of diffusion.

Within the single-phase region (between peritectoid decomposition and solidus), undistorted tetragonal powder could not be detected conclusively by powder diffraction. The addition of excess sulfur results in smaller splitting of the tetragonal $(11l)$ peaks, indicating a smaller distortion and possibly a decrease in sulfur deficiency. It is possible that under extremely precise conditions (near $x = 0.35$ and $T = 900$°C) tetragonal powder may be synthesized. At $x = 0.30$ and $T = 900$°C, the measured $\beta \approx 90.1°$ is extremely close to 90.0°, with the $(11l)$ doublets appearing as broad single peaks. Deconvolution of these peaks, however, always yields two peaks.

The magnetic susceptibility data indicate antiferromagnetic behavior for $BaCoS_{2-\delta}$ with $x = 0$ and $x = 0.1$. As the sulfur content decreases, the Curie constant C and μ_{eff}/Co increase. For $x = 0.1$ the data suggest that Co^{2+} is spin $\frac{1}{2}$ and $g = 2.11$, and for $x = 0$ the g factor is somewhat higher (2.47) assuming spin $\frac{1}{2}$. In this latter case, a mixed Co^{2+}/Co^{+} mixture may be more realistic. For Co^{2+}, $g > 2$ is quite common in pseudo-octahedral environments (13); however, it is completely clear from these data that the Co^{2+} d^7 ion is in the low spin state. An independent neutron

diffraction experiment done on single crystals also revealed spin $\frac{1}{2}$, antiferromagnetically ordered Co (L. S. Martinson, private communication).

We have conclusively shown that sulfur defects in $BaCoS_{2-\delta}$ decrease with increasing sulfur vapor pressure and that these defects are reflected in the unit cell geometry. We also showed that a heretofore undetected superlattice is present in these compounds. The nature of this superlattice and its connection to the magnetic transition near 300 K are not yet understood. We hope that future studies will lead to an even more detailed model of the atomic and electronic structure of these phases.

CONCLUSION

It has been demonstrated that there exist at least three polymorphs of the Mott insulating phase $BaCoS_2$: two that are stoichiometric with tetragonal and monoclinic (1, 2) symmetry, respectively, and the other monoclinic, potentially sulfur-deficient powder. For polycrystalline $BaCoS_{2-\delta}$, the monoclinic angle depends to some extent on sulfur content. By electron diffraction, at least three classes of superstructures were observed in single crystals; a slope change at $-60°C$ in the lattice constants versus temperature for powder could be due to superstructure formation in the crystallites. Susceptibility measurements followed by a fit to the Curie–Weiss law indicate that the Co spins ($\frac{1}{2}$) antiferromagnetically order at around 310 K. The experimental difficulties associated with the characterization of this phase further demonstrate that $BaCoS_{2-\delta}$, clearly a delicate and elusive phase, should be the subject of further studies.

ACKNOWLEDGMENTS

M.C.G. is grateful to Y. Ijiri for assistance with magnetic susceptibility measurements and to G. R. Kowach for crystallography discussion. M.C.G. acknowledges the Air Force Office of Scientific research for partial financial support. R.B. is very thankful for the help given to him by C. Géyou.

REFERENCES

1. G. J. Snyder, M. C. Gelabert, and F. J. DiSalvo, *J. Solid State Chem.* **113,** 355 (1994).
2. N. C. Baenziger, L. Grout, L. S. Martinson, and J. W. Schweitzer, *Acta Crystallogr. C* **50,** 1375 (1994).
3. H. Y. Hong and H. Steinfink, *J. Solid State Chem.* **5,** 93 (1972).
4. G. J. Snyder, M. E. Badding, and F. J. DiSalvo, *Inorg. Chem.* **31,** 2107 (1992).
5. I. E. Grey and H. Steinfink, *J. Am. Chem. Soc.* **92,** 5093 (1970).
6. P. Ehrlich, "Handbook of Preparative Inorganic Chemistry" (G. Brauer, Ed.), 2nd ed., p. 938. Academic Press, New York, 1963.
7. P. Deniard, M. Evain, J. M. Barbet, and R. Brec, Materials Science Forum, *Trans. Tech. Publ.,* 79–82 (1991).
8. J. Rodriguez-Carvajal, "FULLPROF Manual," ILL Report, 1992.
9. J. Vassiliou, M. Hornbostel, R. Ziebarth, and F. J. DiSalvo, *J. Solid State Chem.* **81,** 208 (1989).
10. G. Sheldrick, *Acta. Crystallogr. A* **46,** 467 (1990); "SHELXTL Version 5 software." Siemens Analytical X-ray Instruments, Inc., Madison, WI 1995.
11. L. S. Martinson, J. W. Schweitzer, and N. C. Baenziger, *Phys. Rev. Lett.* **71**(1), 125 (1993).
12. C. Berthier, Y. Chabre, P. Segranssan, P. Chevalier, L. Trichet, and A. Le Méhauté, *Solid State Ionics* **5,** 379 (1981).
13. A. Abragam and B. Bleaney, "Electron Paramagnetic Resonance of Transition Ions" (W. Marshall and D. H. Wilkinson, Eds.), p. 470. Clarendon, Oxford, 1970.